

Thermally stable oxadiazole-containing polyacetylenes: Relationship between molecular structure and nonlinear optical properties†

Xin Wang,^{ab} Shanyi Guang,^a Hongyao Xu,^{*a} Xinyan Su,^b Junyi Yang,^c Yinglin Song,^c Naibo Lin^a and Xiangyang Liu^d

Received 24th April 2008, Accepted 16th June 2008

First published as an Advance Article on the web 29th July 2008

DOI: 10.1039/b807004k

Two novel high molecular weight functional polyacetylenes bearing oxadiazole groups as pendants, poly(2-(4-decyloxyphenyl)-5-(4-ethynylphenyl)-1, 3, 4-oxadiazole) (**P1**) and poly(2-(4-butyloxyphenyl)-5-(4-ethynylphenyl)-1, 3, 4-oxadiazole) (**P2**) were designed and synthesized by a multistep reaction route. The structures and properties were characterized and evaluated with FTIR, NMR, UV, TGA, GPC, optical-limiting (OL) and nonlinear optical (NLO) analyses. The incorporation of oxadiazole into polyacetylene significantly endows polyacetylenes with higher thermal stability and optical limiting property. The solubility, stereoregularity and optical properties of resultant polyacetylenes are obviously affected by flexible terminal alkoxy chain length. The *cis* olefinic structure content in polyacetylene backbone increases with increasing terminal alkoxy group length. The functional polyacetylene with the higher *cis* olefinic structure content shows higher thermal stability, better optical limiting property and larger third-order nonlinear optical performance. The optical limiting mechanism of resulting polymers was investigated, which is mainly originated from larger excitation state absorption cross-section of molecules to result in reverse saturable absorption.

Introduction

Recently, third-order nonlinear optical (NLO) materials based on π -conjugated structure have received much attention because of their potential applications in optical switching, optical bistability, optical modulator and other all-optical devices.^{1,2} Apart from this, it is also a type of important materials for optical limiting application due to their large nonlinear optical properties, high damage threshold, and ultrafast NLO response.^{3–5}

Polyacetylene (PA) is a typical π -conjugated polymer with high $\chi^{(3)}$. Nevertheless, it is difficult to process because of its nonfusibility and insolubility.^{6–9} Therefore, much attention has been being paid to the synthesis of PA derivatives with good processibility, high thermal stability and large NLO susceptibility.^{10,11} Our previous work has substantiated that incorporation of azobenzene into PAs have endowed resultant polymer with novel optical properties, flexible terminal groups significantly improving solubility of resulting PAs.^{12–15} However, the strong ground state electronic absorption in visible region of azobenzene-containing PAs limits its application in laser limiting field. Therefore, it is very important to design new functional PAs for optical limiting application. Oxadiazole is a well-known

electron-withdrawing chromophore, which shows weak ground state electronic absorption in the visible region wavelengths more than 400 nm,^{11,16} good thermal stability¹⁷ as well as large second order nonlinear susceptibility.^{18,19} Based on Schuling's nonlinear optical theory, the third-order nonlinear optical susceptibility (γ) of molecules depends on γ_e^0 , a term related to the movement of electron, and β , the second-order nonlinear optical susceptibility.²⁰ In this paper, we design and prepare two novel soluble oxadiazole-containing PAs (Scheme 1) by directly incorporation of oxadiazole into polyacetylene mainchain, which is expected that incorporating oxadiazole into PA can endow resulting polymer with high thermal stability, novel optical properties and enhanced third-order nonlinear optical properties, and carefully investigate the relationship between the thermal stability, the optical properties and their molecular structure.

Results and discussion

Scheme 1 illustrates the synthetic procedures used for the preparation of our new polymers. Synthesis details are available in the electronic supplementary information.

Polymerization

We first tried to polymerize the monomers by WCl_6 , TaCl_5 - and MoCl_5 - Ph_4Sn , and MoCl_5 . The polymerization of **6a** and **6b** catalyzed by TaCl_6 - Ph_4Sn , MoCl_5 - Ph_4Sn , MoCl_5 at 80 °C or 60 °C in dioxane or toluene were made to get only trace amount polymeric products, while MoCl_5 for **6a** did not work (Table 1, runs 1–4). The polymerization of **6a** and **6b** in the presence of WCl_6 - Ph_4Sn under nitrogen for 24 h produced a pale yellow powdery solid in a low yield (Table 1 and Table 2, runs 5–6) with low molecular weight. The reaction product of **6a** from the

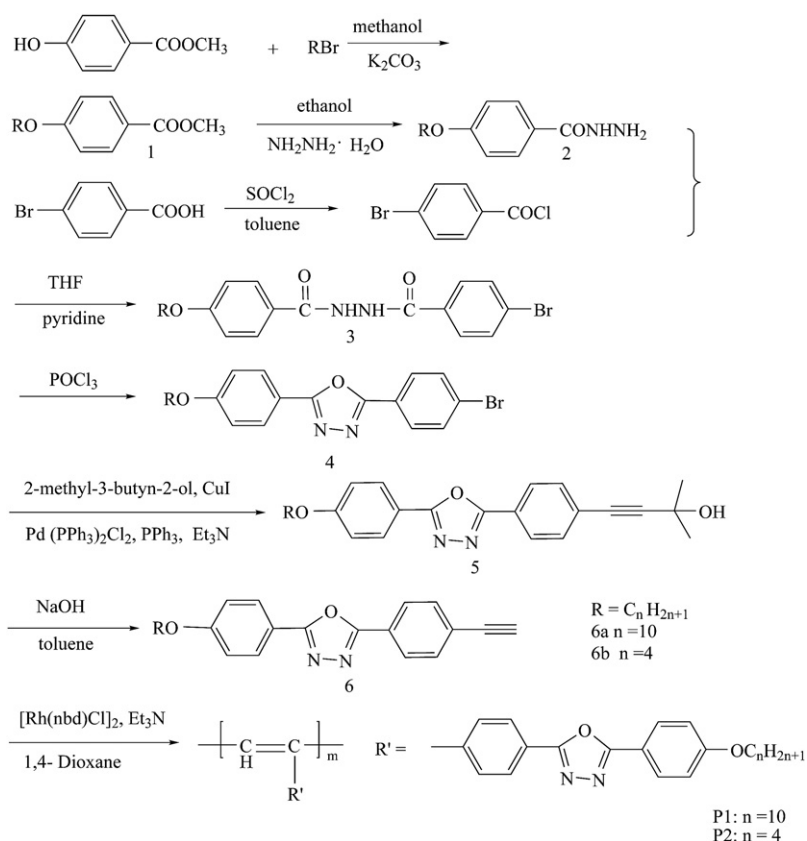
^aCollege of Material Science and Engineering & State Key Laboratory for Modification of Chemical Fibers and Polymer Materials, Donghua University, Shanghai, 200051, China. E-mail: hongyaoxu@163.com; Fax: +86-21-67792874; Tel: +86-21-67792874

^bSchool of Chemistry and Chemical Engineering, Anhui University, Hefei, 230039, China

^cDepartment of Physics, Suzhou University, Suzhou, 215008, China

^dDepartment of Physics, National University of Singapore, Singapore 117542

† Electronic supplementary information (ESI) available: Experimental details. See DOI: 10.1039/b807004k



Scheme 1 Synthetic routes to P1 and P2

WCl₆-Ph₄Sn catalyst does not exhibit absorption peaks of acetylene and olefin protons, but shows a few new peaks in the aromatic proton absorption region, hinting that they had undergone some kind of W-catalyzed trimerization reaction (no triple bond left),^{21–23} which have been confirmed by ¹HNMR

spectra. The polymerized product of **6b** by using WCl₆-Ph₄Sn as catalyst was not further investigated due to its poor solubility.

It is wondrously found that the [Rh(nbd)Cl]₂-Et₃N catalyst worked for the polymerization of **6a** and **6b** in high yield, and the results are listed in Table 1 (run 7–9) and Table 2 (run 7–9),

Table 1 Polymerization summary of **6a**

Run	Catalyst	Temp (°C)	Solvent	Yield (%)	M _w ^e	M _w /M _n ^e
1	MoCl ₅ -Ph ₄ Sn ^a	60	Dioxane	trace		
2	TaCl ₅ -Ph ₄ Sn ^b	80	Toluene	trace		
3	MoCl ₅ -Ph ₄ Sn ^b	60	Toluene	trace		
4	MoCl ₅ ^c	60	Toluene	0		
5	WCl ₆ -Ph ₄ Sn ^b	60	Toluene	25	3200	1.07
6	WCl ₆ -Ph ₄ Sn ^b	60	Dioxane	21	3210	1.04
7	[Rh(nbd)Cl] ₂ -TEA ^d	60	Toluene	92	14300	1.30
8	[Rh(nbd)Cl] ₂ -TEA ^d	60	Dioxane	93	25400	1.71
9	[Rh(nbd)Cl] ₂ -TEA ^d	30	Dioxane	89	25300	1.54

^a Carried out under nitrogen for 6 h; [M]₀ = 0.20M, [cat.] = [cocat.] = 0.020 M. ^b Carried out under nitrogen for 24 h; [M]₀ = 0.20M, [cat.] = [cocat.] = 0.020 M. ^c Carried out under nitrogen for 24 h; [M]₀ = 0.20M, [cat.] = 0.020 M. ^d Carried out under nitrogen for 6 h; [M]₀ = 0.20M, [cat.] = 0.0020M, [cocat.] = 0.0040M. ^e Determined by GPC in THF (calibration: polystyrene).

Table 2 Polymerization summary of **6b**

Run	Catalyst	Temp (°C)	Solvent	Yield (%)	M _w ^e	M _w /M _n ^e
1	TaCl ₅ -Ph ₄ Sn ^a	80	Toluene	Trace		
2	MoCl ₅ -Ph ₄ Sn ^b	60	Dioxane	Trace		
3	MoCl ₅ -Ph ₄ Sn ^a	60	Toluene	Trace		
4	MoCl ₅ ^c	60	Toluene	Trace		
5	WCl ₆ -Ph ₄ Sn ^a	60	Dioxane	24	2210	1.24
6	WCl ₆ -Ph ₄ Sn ^a	60	Toluene	26	3160	1.04
7	[Rh(nbd)Cl] ₂ -TEA ^d	30	Toluene	91	16900	1.52
8	[Rh(nbd)Cl] ₂ -TEA ^d	60	Dioxane	92	29300	1.36
9	[Rh(nbd)Cl] ₂ -TEA ^d	30	Dioxane	91	32700	1.32

^a Carried out under nitrogen for 24 h; [M]₀ = 0.20M, [cat.] = [cocat.] = 0.020 M. ^b Carried out under nitrogen for 6 h; [M]₀ = 0.20M, [cat.] = [cocat.] = 0.020 M. ^c Carried out under nitrogen for 24 h; [M]₀ = 0.20M, [cat.] = 0.020 M. ^d Carried out under nitrogen for 6 h; [M]₀ = 0.20M, [cat.] = 0.0020 M, [cocat.] = 0.0040M. ^e Determined by GPC in THF (calibration: polystyrene).

respectively. All polymerization using $[\text{Rh}(\text{nbd})\text{Cl}]_2\text{-Et}_3\text{N}$ as a catalyst was carried out under nitrogen for 6 h, to yield black yellow or yellow solids. To optimize the polymerization process, we studied the polymerizations of **6a** and **6b** under different reaction temperature and solvent, finding that the resulting polymers showed the higher molecular weight and yield (Table 1, runs 8–9; Table 2, runs 8–9) when polymerization was carried out in dioxane at 60 °C.

Solubility

We first synthesized polyacetylene containing diphenyl oxadiazole chorophore and found that polyacetylene containing diphenyl oxadiazole chorophore is insoluble by directedly incorporation of diphenyl oxadiazole chorophore into polyacetylene mainchain. However, we have found that substituent of flexible terminal group effectively improves solubility of resultant polymers in our previous azobenzene-containing PA.¹⁴ Thus, we designed and synthesized oxadiazole functionalized polyacetylenes with flexible terminal group. It is found that the solubility of resultant PAs is obviously improved and affected by the length of the flexible alkoxy chain length, and solubility of resultant PAs increases with increasing the chain length of flexible terminal alkoxy group. For example, polyacetylene containing diphenyl oxadiazole chorophore without flexible terminal alkoxy chain is insoluble, **P2** with flexible terminal alkoxy group ($n = 4$) is partially soluble in common organic solvent such as THF, CHCl_3 , toluene and dioxane while **P1** with longer flexible terminal alkoxy group ($n = 10$) completely soluble in above common organic solvents. This observation will provide important foundation for molecular design of soluble functional polyacetylenes.

Structural characterization

The structures of **P1** and **P2** were characterized by spectroscopic techniques, and both gave satisfactory data corresponding to their expected molecular structures. The FTIR spectra of **6a** and **P1** are shown in Fig. 1 As can be seen in Fig. 1, **6a** clearly exhibits a strong characteristic absorption band near 3272 cm^{-1} , due to

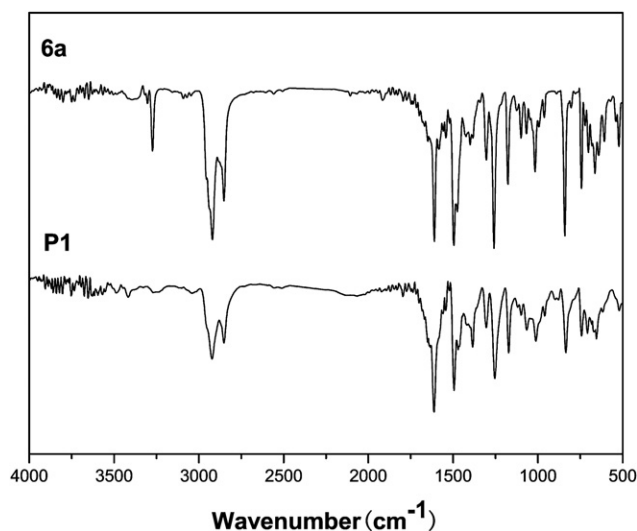


Fig. 1 Fig. 1 FT-IR (KBr pellet) spectra of **6a** and **P1** (Table 1, run 8).

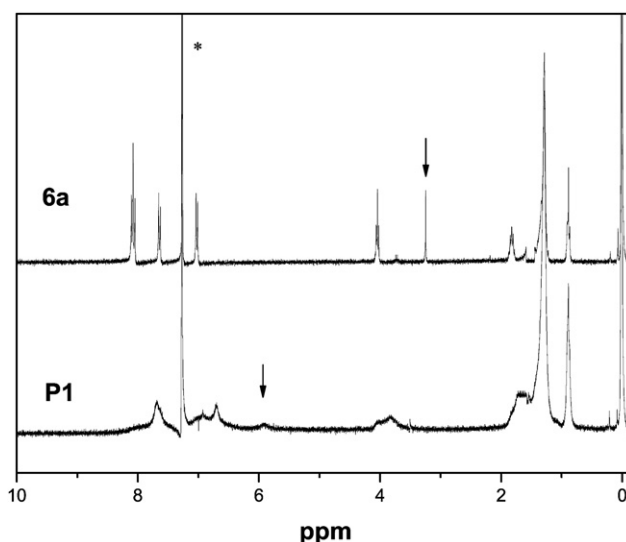


Fig. 2 $^1\text{H NMR}(\text{CDCl}_3)$ spectra of **6a** and **P1** (Table 1, run 8). The solvent peaks are marked with asterisks.

the $\equiv\text{C-H}$ stretching vibration in the monosubstituted acetylene molecules. However, the characteristic ν_s ($\equiv\text{C-H}$) absorption band disappeared in the spectrum of **P1** (Table 1, run 8) and the relative intensity of the stretching band at 1611 cm^{-1} in **P1** significantly increases, which is assigned to $\text{C}=\text{C}$ group, indicating that $\text{C}\equiv\text{C}$ in the monomer has changed into $\text{C}=\text{C}$ group in the polymer and the Rh catalyst has initiated the polymerization of acetylene. The similar results were also observed in spectrum of **P2**.

Fig. 2 shows the $^1\text{H NMR}$ spectra of **6a** and **P1**. The absorption peak of the acetylene proton in **6a** is located at δ 3.25 ppm as a singlet peak, but completely disappears in the spectrum of its polymer **P1**. Alternatively, **P1** shows a broad peak at δ 5.9–6.68 ppm corresponding to the olefin and aromatic protons absorption, which further proves the changing $\text{C}\equiv\text{C}$ to $\text{C}=\text{C}$. The $^1\text{H NMR}$ analysis also provided valuable information of the stereoregularity of the resulting PAs. As shown in Fig. 2, a new *cis* olefin absorption peak (δ 5.92 ppm) appears in the spectrum of **P1**.^{21,23} Based on the Eq (1) used by Tang and Xu for evaluating the stereostructure of the PA derivative,^{14,24} we calculate the *cis* content of the polymers based on the following equation:

$$\text{cis content}(\%) = [A_{5.92}/(A + A_{5.92})/9] \times 100 \quad (1)$$

where $A = A_{7.69} + A_{6.93} + A_{6.68}$, corresponding to the peak areas of the eight aryl protons of the polymers and the peak areas of *trans* olefinic proton, and $A_{5.92}$ corresponds to the peak areas of *cis* olefinic proton. Then, the *cis* olefin contents can be estimated based on integration areas of the peak, i.e., the *cis* contents of **P1** and **P2** are 93.1% and 81.8 %, respectively. The increase of *cis* content of **P1** compared with **P2** may be caused by the *cis-trans* isomerization during the polymerization due to the higher steric hindrance of longer alkoxy chain.^{21,23,25–28}

Optical properties

The photophysical characteristics of the **P1** and **P2** were studied by UV-vis absorption in THF solutions. The absorption spectra

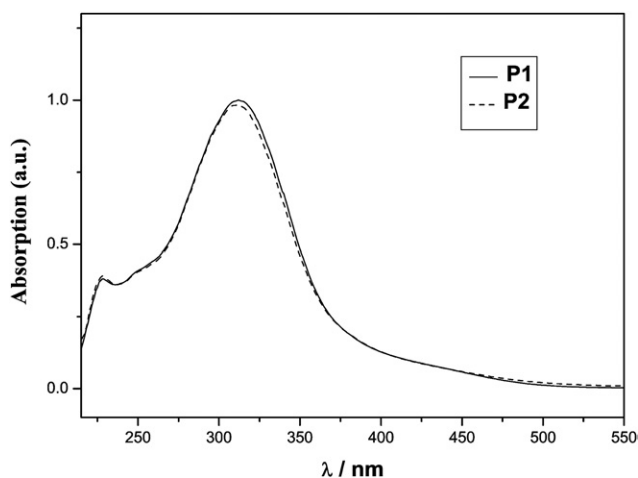


Fig. 3 UV-vis absorption spectra of **P1** (Table 1, run 8) and **P2** (Table 2, run 8) in THF solutions with a concentration of 1×10^{-5} M.

of **P1** and **P2** in THF are given in Fig. 3. **P1** shows a strong absorption at 312 nm, which is attributable to the oxadiazole chromophore units, and the absorption at 400 nm with weak intensity may result from the absorption of the conjugated backbone of PA.^{11,29} The UV-vis absorption spectrum of **P2** is similar to that of **P1** and the maximum absorption is at 311 nm. In addition, the E_{gs} of **P1** and **P2** from the absorption edge of solution samples are 3.30 and 3.33 eV, respectively,¹⁹ indicating the ground-state electronic transitions are little affected by alkoxy chain length.

Thermal properties

It is well known that poly(1-alkyne)s such as poly(1-butyne) and poly(1-hexyne), are so unstable that even isolation process of the polymer products from the polymerization reactions leads to degradation.^{25,30} However, the two polymers exhibit good thermal stability. As shown in Fig. 4, the T_{d5} (weight loss 5%) of **P1** and **P2** are 353 and 346 °C, respectively, indicating that the incorporation of rigid diaryl-oxadiazole group into poly(1-

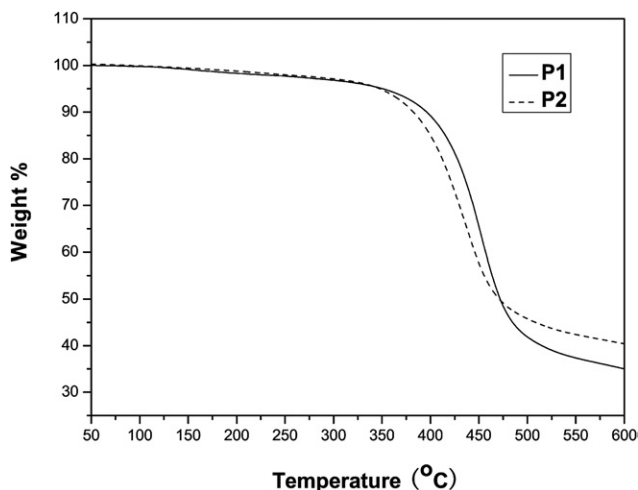


Fig. 4 TGA thermograms of **P1** (Table 1, run 8) and **P2** (Table 2, run 8) measured under nitrogen at a heating rate of 10 °C /min.

alkyne)s has endowed the polymers with high thermal stability. It may be due to the ‘jacket effect’ of the aromatic oxadiazole pendants, namely, the rigid aromatic oxadiazole groups may have formed a protective ‘‘jacket’’ via the strong electronic interactions among the polarized aromatic oxadiazole side chains, shielding the polymer main chains from thermal attack. Similar phenomenon is also found by Tang and our previous work.^{14,19,26,30,31} Simultaneously, it is also found that the thermal stability of resultant polymers is affected by stereoregularity of PA main chain. The thermal stability increases with the increase of *cis* olefin content of polymer, implying that thermal stability could be adjusted by alkoxy chain length. It is consistent with that found in Tang and our previous work.^{19,26}

Optical limiting properties

Fig. 5 shows the optical responses of **P1** ($c = 2.2$ mg/mL, $T = 67\%$), **P2** ($c = 1.8$ mg/mL, $T = 67\%$) along with that of PPA ($c = 4.6$ mg/mL, $T = 67\%$) solutions to 532 nm laser pulses. It can be seen from Fig 5 that, at very low input fluence, the output fluence of all the solutions linearly increases with the incident fluence, obeying the Beer-Lambert law, but at high input fluence, the transmittance of **P1** and **P2** solution decreased, and a nonlinear relationship is observed between the output and input fluence, showing significant OL property. In contrast, the transmittance of the PPA solution continually increases instead of decrease due to the laser induced photolysis of the PA chains,³² indicating that the incorporation of oxadiazole endows PA with novel OL property. Simultaneously, we measured the UV-vis absorption spectrum of the **P1** and **P2** solutions before and after the laser irradiation and found that the pattern and its intensity of UV-vis absorption spectra have almost no change, hinting that the **P1** and **P2** possesses well photostability.

Furthermore, it is also seen that the transmitted fluence of the **P1** solution starts to deviate from linearity when the incident fluence reaches 0.625 J/cm² (defined as limiting threshold, i.e., the incident fluence at which the output fluence starts to deviate from linearity). With a further increase in the incident fluence, the

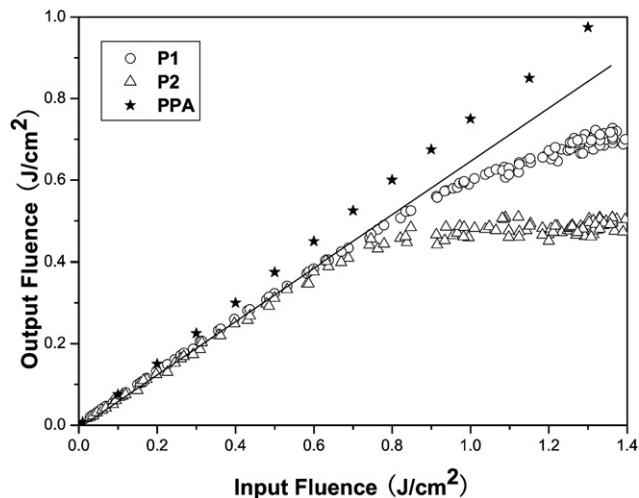


Fig. 5 Optical limiting properties of **P1** and **P2** solution (**P1**: Table 1, run 8 and **P2**: Table 2, run 8) with a linear transmission of 67%. Data for PPA with the same transmission are given for comparison.

transmitted fluence reaches a plateau and is saturated at 0.454 J/cm² (defined as the limiting amplitude, i.e., the maximum output intensity). However, the limiting amplitude value of **P2** is 0.713 J/cm². The result suggests **P1** with longer terminal alkoxy chain and higher *cis* olefin content exhibits better OL performance than **P2** with shorter terminal alkoxy chain and lower *cis* olefin content.

The OL mechanisms of organic compounds are often based on two-photon absorption (TPA) or reverse saturable absorption (RSA). Generally, TPA-based OL effect can be yielded in principle under the laser irradiation of picosecond or shorter pulses. RSA is achieved on a nanosecond or longer time scale, rather than a picosecond time scale, owing to the different excited state lifetimes involved in a multilevel energy process.³³ In the present work, the molecules are excited by the laser with 4 ns pulse width at 532 nm wavelength and the transmittance of all these polymers' solution decreases with the increase of the incident fluence. Therefore, we can consider that the OL properties of **P1** and **P2** may be originated from RSA.

The OL property of RSA molecules can be evaluated by the ratio of the excited-state absorption cross-section (σ_{ex}) to the ground state absorption cross-section (σ_0) of molecules, which was defined as $\sigma_{\text{ex}}/\sigma_0 = \ln T_{\text{sat}}/\ln T_0$. T_{sat} is the saturated transmittance for high degrees of excitation.³⁴ The larger value of $\sigma_{\text{ex}}/\sigma_0$, the better OL performance. In our experimental set up, although we are unable to reach the saturable transmittance for these compounds, we can use the transmittance at 1.4 J/cm² to calculate the lowest bound for $\sigma_{\text{ex}}/\sigma_0$. Based on the experiment data illustrated in Fig. 5, the calculated values of $\sigma_{\text{ex}}/\sigma_0$ for **P1** and **P2** are 2.81 and 1.68, respectively, further confirming that their OL mechanism are mainly originated from large excitation state absorption cross-section to result in reverse saturable absorption.

Nonlinear optical properties

The nonlinear absorption coefficients of PAs were measured by using Z-scan technique. The results of Z-scan with and without an aperture showed that these PAs have both nonlinear absorption (Fig. 6-A) and nonlinear refraction (Fig. 6-B).

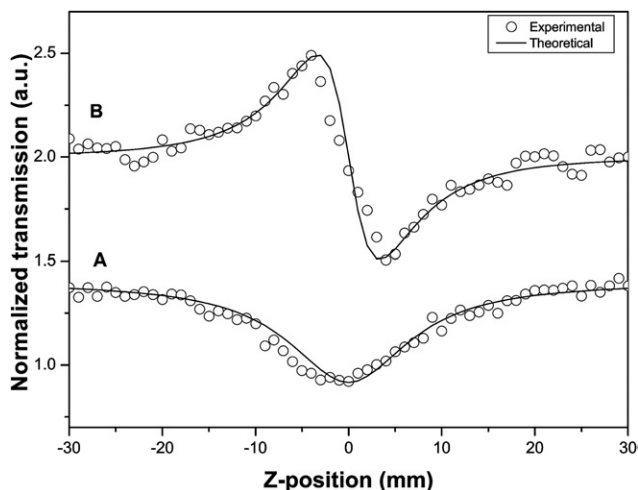


Fig. 6 Z-scan data of (A) open and (B) closed apertures of **P1**. (Table 1, run 8).

Table 3 Summary of optical limiting and nonlinear optical properties of **P1** (Table 1, run 8) and **P2** (Table 2, run 8)

	OL Amplitude (J/cm ²) ^a	NLO Properties ^b		
		β ($\times 10^{-11}$ m/W)	n_2 ($\times 10^{-19}$ m ² /W)	$\chi^{(3)}$ ($\times 10^{-12}$ esu)
P1	0.454	8.54	16.10	4.67
P2	0.713	4.75	6.94	2.15

^a Maximum output intensity. ^b Measured by the Z-scan technique with an 13-ns Nd:YAG laser system at a 1-Hz repetition rate and a 532-nm wavelength.

In theory, the normalized transmittance for the open aperture can be written as:³⁵

$$T(z, s = 1) = \sum_{m=0}^{\infty} \frac{[-q_0(z, 0)]^m}{(m+1)^{3/2}} \text{ for } |q_0| < 1 \quad (2)$$

where $q_0(z) = \alpha_2 I(t) L_{\text{eff}} / (1 + Z^2/Z_0^2)$, α_2 is the nonlinear absorption coefficient, $I_0(t)$ is the intensity of laser beam at focus ($z = 0$), $L_{\text{eff}} = |1 - \exp(-\alpha_0 L)|/\alpha_0$ is the effective thickness with α_0 the linear absorption coefficient and L the sample thickness, z_0 is the diffraction length of the beam, and z is the sample position. Thus, the nonlinear absorption coefficients of the polymers can be determined by fitting the experimental data using Eq. (2).

The normalized transmission for the closed aperture Z-scan is given by the following:³⁵

$$T = 1 + \frac{4\Delta\phi_0 x}{(x^2 + 9)(x^2 + 1)} \quad (3)$$

where $x = z/z_0$ and $\Delta\phi$ is on-axis phase change caused by the nonlinear refractive index of the sample and $\Delta\phi = 2\pi I_0(1 - e^{-L\alpha_0})n_2/\lambda\alpha_0$. Thus, the nonlinear refractive coefficients of the polymers can be determined by fitting the experimental data using Eq.(3).

The $\chi^{(3)}$ can be calculated by Eq.(4):³⁵

$$|\chi^{(3)}| = \sqrt{\left| \frac{cn_0^2}{80\pi} n_2 \right|^2 + \left| \frac{9 \times 10^8 \epsilon_0 n_0^2 c^2}{4\pi\omega} \beta \right|^2} \quad (4)$$

where ϵ_0 is the permittivity of vacuum, c is the speed of light, n_0 is the refractive index of the medium and $\omega = 2\pi c/\lambda$. Therefore, the results can be calculated and are listed in Table 3. From Table 3, the nonlinear absorption coefficients of the **P1** and **P2** are 8.54×10^{-11} and 4.75×10^{-11} m/W, respectively. The β values of **P1** and **P2** (9.5×10^{-11} m/W)¹⁹ increased with the *cis* olefin content of those increasing. In addition, the nonlinear susceptibilities $\chi^{(3)}$ of the **P1** and **P2** are 4.67×10^{-12} and 2.15×10^{-12} esu, respectively, which enhanced with an increase in the alkoxy chain length.¹⁴

Conclusion

Two functional PAs containing oxadiazole groups with different terminal alkoxy group are designed and prepared by a multistep reaction route. The incorporation of rigid aromatic oxadiazole group into polyacetylenes had endowed the polyacetylenes with high thermal stability, which may be owing to 'jacket effect' of the aromatic oxadiazole pendants. The solubility of resultant

polymers can be adjusted by varying terminal alkoxy chain length. The oxadiazole-containing PA with longer terminal alkoxy group chain shows better solubility than PA with shorter terminal alkoxy chain. Simultaneously, the stereoregularity and properties of the resulting PAs is also significantly affected by terminal alkoxy group chain length. The *cis* olefinic structure content in PA backbone increases with increasing terminal alkoxy group length, which is mainly attributed to the more difficult *cis-trans* isomerization during polymerization due to the larger stereo-hindrance of alkoxy chain. Polymer with higher *cis* olefinic structure content exhibits higher thermal stability, better optical limiting properties and nonlinear optical property. The OL mechanism are mainly originated from larger excitation state absorption cross-section to result in reverse saturable absorption. This work provides further understanding of relationship between molecular structure and their optical properties of functional PAs and paves the new way for designing new soluble functional PAs with high thermal stability and well optical limiting property.

Acknowledgements

This research was financially supported by the National Natural Science Fund of China (Grant Nos. 90606011 and 50472038), Ph.D. Program Foundation of Ministry of Education of China (No.20070255012) and Shanghai Leading Academic Discipline Project (No. B603).

References

- 1 Y. Suzuki, K. Komatsu, T. Kaino and Y. Honda, *Opt. Mater.*, 2003, **21**, 521–524.
- 2 Y. Shi, W. Lin, D. J. Olson, J. H. Bechtel, H. Zhang, W. H. Steier, C. Zhang and L. R. Dalton, *Appl. Phys. Lett.*, 2000, **77**, 1–3.
- 3 M. Samoc, A. Samoc and B. Luther-Davies, *Synth. Met.*, 2000, **109**, 79–83.
- 4 B. Li, H. Wu, W. Yi, C. Gao and X. Li, *Synth. Met.*, 2005, **155**, 146–149.
- 5 M. Hotzel, S. Urban, D. A. M. Egbe, T. Pautzsch and E. Klemm, *J. Opt. Soc. Am. B: Opt. Phys.*, 2002, **19**, 2645–2649.
- 6 W. S. Fann, S. Benson, J. M. Madey, S. Etemad, G. L. Baker and F. Kajar, *Phys. Rev. Lett.*, 1989, **62**, 1492–1495.
- 7 H. Shirakawa, *Angew. Chem., Int. Ed.*, 2001, **40**, 2574–2580.
- 8 J. W. Y. Lam and B. Z. Tang, *Acc. Chem. Res.*, 2005, **38**, 745–754.
- 9 G. P. Agrawal, C. Cojan and C. Flytzanis, *Phys. Rev. B*, 1978, **17**, 776–789.
- 10 J. Huang, C. Li, Y. J. Xia, X. H. Zhu, J. Peng and Y. Cao, *J. Org. Chem.*, 2007, **72**, 8580–8583.
- 11 S. H. Jin, M. Y. Kim, J. Y. Kim, K. Lee and Y. S. Gal, *J. Am. Chem. Soc.*, 2004, **126**, 2474–2480.
- 12 S. Yin, H. Xu, X. Su, L. Wu, Y. Song and B. Z. Tang, *Dyes Pigm.*, 2007, **75**, 675–680.
- 13 S. Yin, H. Xu, W. Shi, L. Bao, Y. Gao, Y. Song and B. Z. Tang, *Dyes Pigm.*, 2007, **72**, 119–123.
- 14 S. C. Yin, H. Y. Xu, X. Y. Su, G. Li, Y. L. Song, J. W. Y. Lam and B. Z. Tang, *J. Polym. Sci., Part A: Polym. Chem.*, 2006, **44**, 2346–2357.
- 15 S. Yin, H. Xu, W. Shi, Y. Gao, Y. Song, J. W. Y. Lam and B. Z. Tang, *Polymer*, 2005, **46**, 7670–7677.
- 16 C. B. He, Y. Xiao, J. C. Huang, T. T. Lin, K. Y. Mya and X. H. Zhang, *J. Am. Chem. Soc.*, 2004, **126**, 7792–7793.
- 17 H. H. Sung and H. C. Lin, *Macromolecules*, 2004, **37**, 7945–7954.
- 18 S. H. Mashraqui, R. S. Kenny, S. G. Ghadigaonkar, A. Krishnan, M. Bhattacharya and P. K. Das, *Opt. Mater.*, 2004, **27**, 257–260.
- 19 X. Wang, J. Wu, H. Xu, P. Wang and B. Tang, *J. Polym. Sci., Part A: Polym. Chem.*, 2008, **46**, 2072–2083.
- 20 A. Schuling, *Chem. Phys. Lett.*, 1967, 195–199.
- 21 Y. Fujita, Y. Misumi, M. Tabata and T. Masuda, *J. Polym. Sci., Part A: Polym. Chem.*, 1998, **36**, 3157–3136.
- 22 M. Haussler, J. Liu, R. Zheng, J. W. Y. Lam, A. Qin and B. Z. Tang, *Macromolecules*, 2007, **40**, 1914–1925.
- 23 M. Tabata, Y. Tanaka, Y. Sadahiro, T. Sone, K. Yokota and I. Miura, *Macromolecules*, 1997, **30**, 5200–5204.
- 24 M. Tabata, T. Sone, Y. Sadahiro, K. Yokota and Y. Nozaki, *J. Polym. Sci., Part A: Polym. Chem.*, 1998, **36**, 217–223.
- 25 B. Z. Tang, X. Kong, X. Wan, H. Peng, W. Y. Lam, X. D. Feng and H. S. Kwok, *Macromolecules*, 1998, **31**, 2419–2432.
- 26 B. Z. Tang, X. Kong, X. Wan and X. D. Feng, *Macromolecules*, 1997, **30**, 5620–5628.
- 27 C. H. Ting, J. T. Chen and C. S. Hsu, *Macromolecules*, 2002, **35**, 1180–1189.
- 28 X. Kong, J. W. Y. Lam and B. Z. Tang, *Macromolecules*, 1999, **32**, 1722–1730.
- 29 J. W. Y. Lam, Y. Dong, H. S. Kwok and B. Z. Tang, *Macromolecules*, 2006, **39**, 6997–7003.
- 30 J. W. Y. Lam, Y. Dong, K. K. L. Cheuk, J. Luo, Z. Xie, H. S. Kwok, Z. Mo and B. Z. Tang, *Macromolecules*, 2002, **35**, 1229–1240.
- 31 S. C. Yin, H. Y. Xu, M. Fang, W. F. Shi, Y. C. Gao and Y. L. Song, *Macromol. Chem. Phys.*, 2005, **206**, 1549–1557.
- 32 B. Z. Tang and H. Xu, *Macromolecules*, 1999, **32**, 2569–2576.
- 33 W. F. Sun, M. M. Bader and T. Carvalho, *Opt. Commun.*, 2003, **215**, 185–190.
- 34 J. W. Perry, K. Mansour, S. R. Marder, K. J. Perry, J. Daniel Alvarez and I. Choong, *Opt. Lett.*, 1994, **19**, 625–627.
- 35 M. S. BaHae, A. A. Said, T. H. Wei, D. J. Hagan and E. W. V. Stryland, *IEEE J. Quantum Electron.*, 1990, **26**, 760–769.